J Radioanal Nucl Chem (2013) 295:2049–2057
DOI 10.1007/s10967-012-2201-4

Distribution and behavior of some radionuclides associated with the Trinity nuclear test

Jeremy J. Bellucci · Christine Wallace · Elizabeth C. Koeman · Antonio Simonetti · Peter C. Burns · Jeremy Kieser · Eli Port · Terri Walczak

Received: 14 August 2012 / Published online: 18 September 2012

Abstract The activities of ^{133}Ba, ^{137}Cs, ^{152}Eu, ^{154}Eu, ^{155}Eu, ^{239}Pu, and ^{241}Am were determined by gamma spectroscopy on the largest sample set (n = 49) of bulk trinitite to date. The range in activity for all isotopes is large. For example, the activity of ^{241}Am (normalized to the time of detonation) ranges between 1 and 42 Bq/g. Comparison of activities for isotopes derived from the device, ^{241}Am versus ^{137}Cs, ^{155}Eu, and ^{239}Pu, indicate positive trends. Correlations were not observed between the activities of the soil-derived activation products ^{152}Eu and ^{154}Eu and the radioisotopes from the device. The calculated ratio of fission products (^{155}Eu/^{137}Cs) is 0.012 ± .006 (1σ, n = 3), which is lower than predicted for the thermal neutron-induced fission of ^{239}Pu (~0.03). This discrepancy may be attributed to the spontaneous fission of the natural U tamper resulting in mixing between fission products from ^{239}Pu and ^{235}U. The spatial distribution of the trinitite samples relative to ground zero has been modeled based on the activity of ^{152}Eu. The calculated distances do not correlate with any of the activities for the radioisotopes investigated here, and suggest a relatively homogeneous distribution. However, trinitite samples with the highest activities for ^{137}Cs, ^{239}Pu, and ^{241}Am yield the shortest calculated distances of 50–60 m away from ground zero.

Keywords Trinitite · Nuclear forensics · Gamma spectroscopy · Radionuclides · Fission and activation products

Introduction

Nuclear proliferation is one of the greatest threats facing civilization today. The behavior and distribution of radioactive isotopes after a nuclear event is of much interest to the nuclear science and security communities. For example, understanding the behavior and distribution of these isotopes after an event is useful in quantifying the extent of environmental contamination and in determining the ideal location for post-detonation forensic investigations. An important first step in establishing protocols for nuclear forensics is to understand and decipher the chemical and isotopic make-up of post-detonation materials at test sites. The primary motivation behind studying materials from historic U.S. weapons test sites is that the chemical and isotopic compositions of materials used for the weapons employed there are relatively well documented. This documentation provides a means to verify any results gained from forensic investigations of post-detonation material. The post-detonation materials created during the first atomic weapon test, Trinity, are available for public research and provide an excellent opportunity for establishing protocols in nuclear forensics.

The Trinity test was conducted at the White Sands Proving Ground just south of Alamogordo, New Mexico. The detonation took place at 5:29:45 a.m. on July 16, 1945

Electronic supplementary material The online version of this article (doi:10.1007/s10967-012-2201-4) contains supplementary material, which is available to authorized users.

J. J. Bellucci (✉) · C. Wallace · E. C. Koeman · A. Simonetti · P. C. Burns
Department of Civil and Environmental Engineering and Earth Sciences, Notre Dame University, Notre Dame, IN 46556, USA
e-mail: jeremy.bellucci@gmail.com

J. Kieser · E. Port · T. Walczak
RSSI 6312, West Oakton Street, Morton Grove, IL 60053-2723, USA

and ushered in the Nuclear Age. The device, Gadget, was an implosion-type design with a "super-grade" ^{239}Pu core produced at the Hanford site (^{240}Pu/^{239}Pu = 0.0128–0.016 mol/mole, [1, 2]). Prior to the test, the Gadget was hoisted onto a steel tower to an elevation of 30.5 m. Upon detonation, a ~21-kiloton explosion created a fireball with a height of 15.2–21.3 km and a temperature of ~8,430 K [3]. Materials from the bomb, the test site, and the underlying geology were entrained by this fireball, and formed a green, glassy material known as trinitite [1, 3–5]. The blast produced a circular, glassy layer of trinitite that was ~370 m in diameter and centered on the tower [5]. Three types of anthropogenic radioisotopes are distributed in a nuclear explosion: un-fissioned fuel and their daughter products (^{239}Pu, ^{240}Pu, ^{241}Am); fission products (^{137}Cs, ^{155}Eu), produced directly by the fission of ^{239}Pu; and activation products (^{133}Ba, ^{152}Eu, and ^{154}Eu), produced by capture of neutrons released during a nuclear reaction. Gamma spectroscopy provides a non-destructive means for the quantification of the specific activities of the aforementioned radionuclides in bulk samples of post-detonation materials, such as trinitite.

Remnants of nuclear fuel

Both un-fissioned fuel and ^{241}Am, a β-decay product from ^{241}Pu ($t_{1/2}$ = 14.4 years), are detectable by gamma spectroscopy. During the high neutron flux produced by the nuclear reaction, ^{241}Pu is created via neutron capture from excess ^{239}Pu by one of two pathways: 1) double (n, γ) to ^{240}Pu and subsequently ^{241}Pu or 2) a single (2n, γ) reaction. The Pu used in the Gadget was of super grade quality, but trace amounts of ^{241}Pu were present in the core of the device [2, 6]. It is more likely, however, that any detectable ^{241}Am is derived from ^{241}Pu that was produced by neutron capture [2].

Table 1 Gamma energies used in determining activity

Nuclide	Energy (KeV)
^{133}Ba	356.01
^{137}Cs	661.66
^{152}Eu	121.7, 344.2, 778.90, 964.08
^{154}Eu	123.07, 723.30, 1,004.76, 1,274.43
^{155}Eu	86.55, 105.31
^{239}Pu	51.62, 129.30, 375.05, 413.71
^{241}Am	59.54

Fission products

Wahl [7] modeled the abundances of fission products formed by the thermal neutron-induced fission of ^{239}Pu, the fuel used in the Gadget, and other fissile nuclei. The result is a bimodal, asymmetric mass distribution, with the relative proportions of fission products depending on the mass number of the isotope undergoing fission and the speed of the impacting neutrons. The mass number of the isotope undergoing fission determines the mass number of the daughter isotopes, largely due to even–odd proton pairing during fission [7]. Therefore, the thermal neutron-induced fission of ^{235}U and ^{239}Pu yield different abundances of fission products [7]. Accordingly, determining the ratios of fission products should provide an immediate way to constrain the type of fuel used in a nuclear device. The two fission products that were detected in this study are ^{137}Cs and ^{155}Eu, which have fission yields of 6.762 and 0.173 %, respectively [7]. Semkow et al. [8] have argued that U in the Gadget device's natural U tamper also underwent fission and contributed ~30 % of the energy associated with the Trinity test. A comparison between the predicted and actual fission product yields should provide insights into whether-or-not

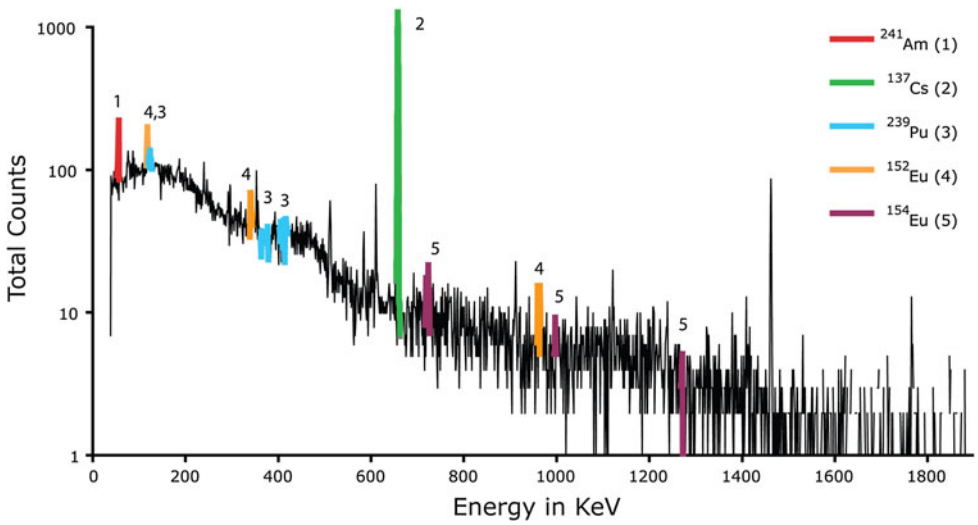

Fig. 1 An example of a typical gamma spectrum. Relevant isotopes are *numbered* and *highlighted*

Table 2 Activities in Bq/g normalized to the time of detonation

Sample	^{241}Am	σ	^{137}Cs	σ	^{152}Eu	σ	^{154}Eu	σ	^{239}Pu	σ	^{133}Ba	σ	^{155}Eu	σ
1-6.37	3.4	0.3	27.8	0.04	20	1	30	2						
1-7.42	9.4	0.3	108.0	0.03	92	2								
1-7.76	1.0	1.6	87.6	0.04	32	2	205	11						
1-3.59	4.8	0.8	38.1	1.12									0.2	0.1
1-5.05	11.4	1.2	43.0	1.08	79	6	56	4	6,710	1,389			0.7	0.1
2-6.00	1.4	0.9	21.9	0.06	35	2								
2-6.10	38.9	0.3	313.5	0.05										
2-6.28	17.3	0.2	178.7	0.03	43	3								
2-3.78	12.1	0.9	63.0	1.32										
3-12.20	19.2	0.0	185.4	0.00	24	1	34	1						
3-14.46	18.6	0.0	215.7	0.01	22	1								
3-5.25	6.5	0.7	50.1	1.28										
4A-3.17	21.1	0.9	145.0	0.14	44	7	332	56						
4A-3.36			28.7	0.23	8	1								
4A-1.95			9.7	0.80										
4B-11.59	2.4	0.1	15.7	0.03	36	1								
4B-7.55	9.3	0.8	53.6	0.08	52	3								
4B-2.65	7.4	1.6	58.5	1.82	56	8								
4B-2.83	18.2	1.9	111.8	2.24	14	1	169	17					1.5	0.3
4C-5.75	14.1	0.2	105.3	0.03	41	3								
4C-8.56	42.0	0.1	89.5	0.03	50	2	507	18						
4C-10.6	2.3	0.3	15.8	0.39	24	2								
4C-5.33	4.9	0.7	37.1	0.98	57	4								
4D-5.10	3.8	0.4	22.8	0.07	30	3								
4D-0.69			30.5	1.89										
4D-10.44	10.4	0.6	87.3	1.05	44	3					42	5		
4D-2.45			29.3	1.29	45	8	186	34						
4D-9.18	2.0	0.4	51.4	0.77	21	2								
4E-1.04	17.7	2.3									27	16	1.0	0.2
4E-10.07	40.0	1.9	370.8	2.59	56	4								
4E-5.22			73.8	1.30	40	5	29	3						
4F-5.37B	15.2	1.0	49.7	0.24	93	8	159	14						
4F-2.36	3.7	1.6	24.3	1.59										
5A-6.06B	42.0	0.2	94.9	0.08	92	4								
5A-6.62	1.8	0.4	14.7	0.06	70	1	120	2						
5A-8.86	11.1	0.2	80.7	0.04	91	1								
5B-10.22	9.0	0.1	78.4	0.03	41	2								
5B-10.4	7.1	0.5	87.8	1.19	51	4								
5B-5.78	11.5	1.0	105.3	1.57	30	5	79	12						
5D-1.57	10.3	2.8	43.8	1.64	11	2	228	32						
5D-1.72	18.4	1.5	130.1	2.80										
5D-1.78	18.7	2.4	95.4	2.33	73	10			13,160	3,843				
5D-1.94	30.7	2.4			96	10	85	9	13,753	2,393				
5D-5.18	0.7	0.4	18.9	0.69	30	3					33	5		
5E-1.50	19.2	2.6	116.1	2.90							110	22		
5E-2.10	7.2	1.1	83.9	1.87										
5E-2.16	19.9	2.9	96.9	2.38	92	11								
5E-2.44			78.5	1.89										

Table 2 continued

Sample	^{241}Am	σ	^{137}Cs	σ	^{152}Eu	σ	^{154}Eu	σ	^{239}Pu	σ	^{133}Ba	σ	^{155}Eu	σ
5F-6.30	13.0	0.1	95.7	0.03	113	1								
5F-7.57	11.1	1.0	132.7	1.55	44	4								

Table 3 Statistics on the activities for each isotope

	^{241}Am	^{137}Cs	^{152}Eu	^{154}Eu	^{239}Pu	^{133}Ba	^{155}Eu
Average	13	85	50	158	11,208	53	0.9
σ	11	72	27	134	3,907	39	0.6
$\%_\sigma$	82	84	55	84	35	73	65
n	44	48	38	14	3	4	4
Max	42	371	113	507	13,753	110	2
Min	1	10	8	29	6,710	27	0.2
Median	11	78	44	140	13,160	38	1

σ was calculated as one standard deviation on the mean for each isotope

there was a significant component of U fission in the Trinity test.

Activation products

The geology at ground zero was subjected to a large neutron flux as a result of the fission of ^{239}Pu (+U). During that flux, isotopes with sufficient activation cross-sections absorbed slow neutrons to produce activation products. The two naturally occurring isotopes of Eu, ^{151}Eu and ^{153}Eu, both undergo a (n, γ) reaction upon interaction with thermal neutrons to produce ^{152}Eu and ^{154}Eu, respectively. Bainbridge [9] measured the flux of neutrons during the Trinity test and observed an exponential decay with increasing distance from ground zero. Although the absorption of neutrons by a nucleus is dependent on several factors including bulk rock/matrix chemistry, previous studies have demonstrated that utilizing the activity of ^{152}Eu provides a method for approximating the spatial context of post detonation samples from ground zero [2, 10].

The activation product ^{133}Ba is produced by the ^{132}Ba (n, γ) reaction. Barium is present in both the nuclear device and the surrounding geology [6, 11]. The Ba within the Gadget was present in the explosives in the form $Ba(NO_3)_2$ and used to initiate the nuclear reaction [6, 8]. Barium is also present in the White Sands Proving Ground in the form of barite ($BaSO_4$; [11]). A barium + sulfur-bearing phase, presumably barite, has also been observed as an intact inclusion present on the melted surface of trinitite [12]. Therefore, ^{133}Ba in trinitite could have multiple sources since it may be the result of neutron activation of Ba-bearing phases in the sand at the White Sands Proving Ground, or attributable to the device; this issue may be resolvable if, for example, the activity of ^{133}Ba is correlated with other bomb-derived isotopes.

Several studies have addressed the incorporation of radionuclides into trinitite on a hand-sample and/or micron scale (e.g., [1, 2, 10]). Although, to date, robust constraints on the large-scale (10–100 s of m) distribution of radionuclides is lacking, and is largely due to the small sample sets investigated (n = 3). The Trinity site was bulldozed in 1954 and the blast surface was consequently buried [13]. As a result of the bulldozing and burial, all trinitite samples lack spatial constraints relative to their exact location during the test. Therefore, other methods, such as specifically utilizing the activity of ^{152}Eu can be employed to produce spatial resolution. This study aims to place a large set (n = 49) of trinitite samples in spatial context and model the distribution and behavior of fission products and radionuclides. The trinitite samples investigated here were purchased from Mineralogical Research Corporation (http://www.minresco.com) and represent 12 different groups based on morphological characteristics (Supplementary Materials).

Methods

All analyses were performed at Radiation Safety Services, Inc. in Morton Grove, Illinois (www.rssi.com). Whole rock samples were placed into a petri dish within a Marinelli container and then placed directly on top of the Ge detector, which results in a sample-to-detector distance of 4–5 mm. Gamma spectra were taken using a DART gamma spectrometer with a 30 % efficiency high-purity Ge (HPGe) detector cooled with liquid nitrogen. The detector

Table 4 Activity of ^{152}Eu (normalized to time of detonation) in Bq/g and calculated distance away from ground zero

Sample	^{152}Eu activity	σ	Calculated distance	σ
1-6.37	20	1	69	5
1-7.42	92	2	51	1
1-7.76	32	2	63	3
1-3.59				
1-5.05	79	6	52	4
2-6.00	35	2	62	3
2-6.10				
2-6.28	43	3	60	5
2-3.78				
3-12.20	24	1	67	2
3-14.46	22	1	68	4
3-5.25				
4A-3.17	44	7	59	10
4A-3.36	8	1	81	8
4A-1.95				
4B-11.59	36	1	61	1
4B-7.55	52	3	57	3
4B-2.64	56	4	56	4
4B-2.83	14	1	74	7
4C-5.75	41	3	60	5
4C-8.56	50	2	58	2
4C-10.6	24	2	67	5
4C-5.33	57	4	56	4
4D-5.10	30	3	64	6
4D-0.69				
4D-10.44	44	3	59	4
4D-2.45	45	8	59	11
4D-9.18	21	2	68	7
4E-1.04				
4E-10.07	56	4	56	4
4E-5.22	40	5	60	7
4F-5.37B	93	8	51	4
4F-2.36				
5A-6.06B	92	4	51	2
5A-6.62	70	1	54	1
5A-8.86	91	1	51	1
5B-10.22	41	2	60	3
5B-10.4	51	4	58	5
5B-5.78	30	5	64	10
5D-1.57	11	2	77	11
5D-1.72				
5D-1.78	73	10	53	8
5D-1.94	96	10	50	5
5D-5.18	30	3	64	7
5E-1.50				
5E-2.10				
5E-2.16	92	11	51	6
5E-2.44				
5F-6.30	113	1	49	0
5F-7.57	44	4	59	6

and sample were housed in a 9.5 cm thick vessel with graded Cu & Pb shielding. The DART gamma spectrometer is an 8 k channel, multichannel analyzer, which provides functionality required to support a HPGe detector in a gamma spectrometer system. The DART system includes a computer controlled amplifier, a bias supply, a spectrum stabilizer, an analog-to-digital circuit, data memory, and a ratemeter. Detection and data reduction were performed with an Ortec GEM-30185 HPGe detector and Ortec GammaVision software, respectively.

Each sample was measured for 1 h, where total counts were reported for each channel. Activities for each isotope were taken at the energies listed in Table 1 and were calculated by determining the area under each peak, after subtracting the background. To correct for sum and cascade peaks, the software uses a true coincidence correction factor, designed to correct for all pulses removed from the full-energy peak. The software calculates the sum peak factor during the efficiency calibration. To perform the efficiency calibration an Eckert & Ziegler, NIST certified multi-nuclide standard (#1369-10) was counted for 48 h. After counting, data are used to best fit a 6-term polynomial efficiency curve incorporating the geometry correction for a Ge-detector and samples in a Marinelli container ($\sim$0.7). Errors in the activities were determined by counting statistics and any associated errors due to small variations in sample geometry are incorporated in the relatively large error estimates reported here. A typical gamma energy spectrum is shown in Fig. 1, with important isotopes numbered and highlighted.

Determining a spatial model

A spatial distribution was established for the trinitite samples investigated here based on the methodologies previously outlined in Belloni et al. [10] and Parekh et al. [2]. Calculated distances away from ground zero were determined by using the calculated slow neutron flux determined by the following input parameters: (1) the activity of ^{152}Eu; (2) the cross section of ^{151}Eu; (3) the half-life of ^{152}Eu; (4) the isotopic abundance of ^{151}Eu; (5) the concentration of Eu in the sand; (6) the atomic mass of Eu; and (7) an approximation of the contribution of fast neutrons. The contribution of fast neutrons to the process of activation should be small, and

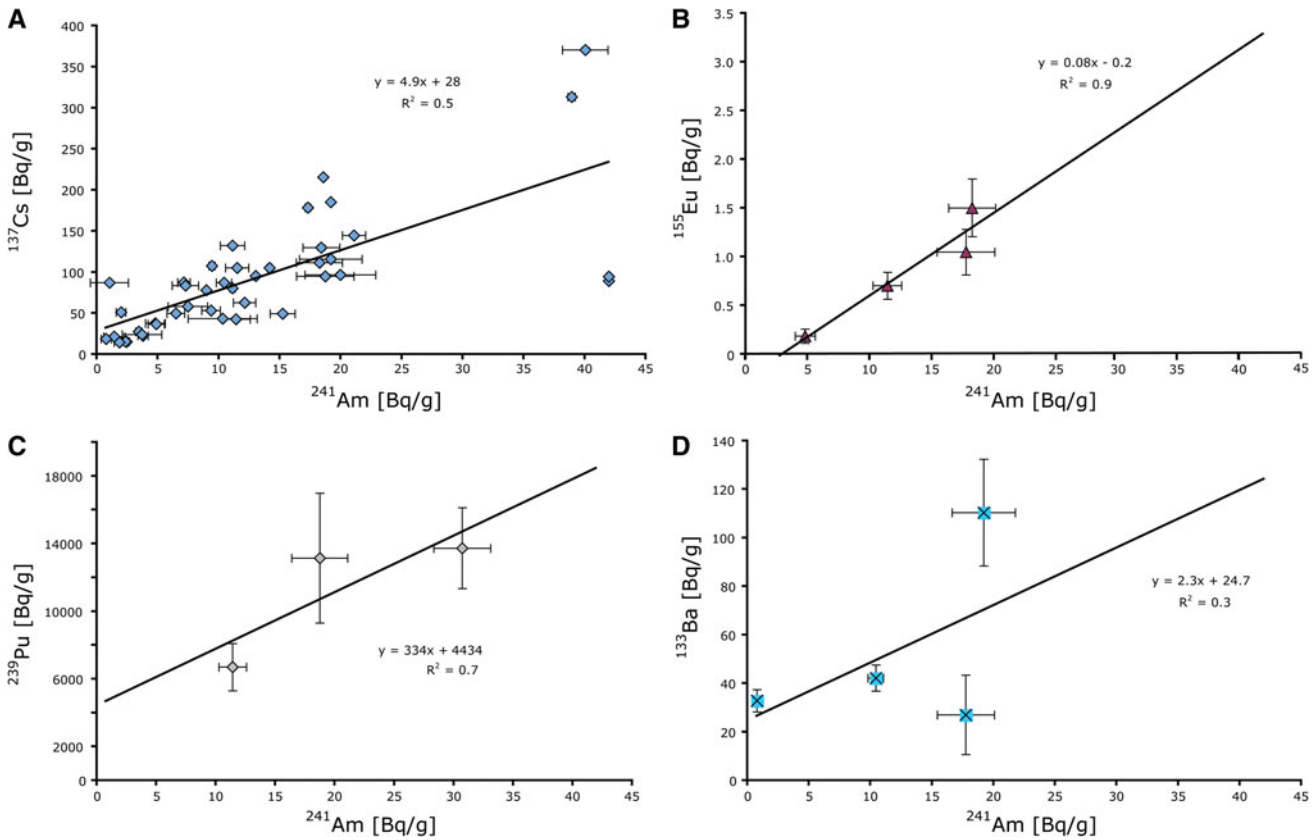

Fig. 2 ^{241}Am versus ^{133}Ba, ^{137}Cs, ^{155}Eu, and ^{239}Pu. *Error bars* are 1σ. Units are Bq/g normalized to the time of detonation

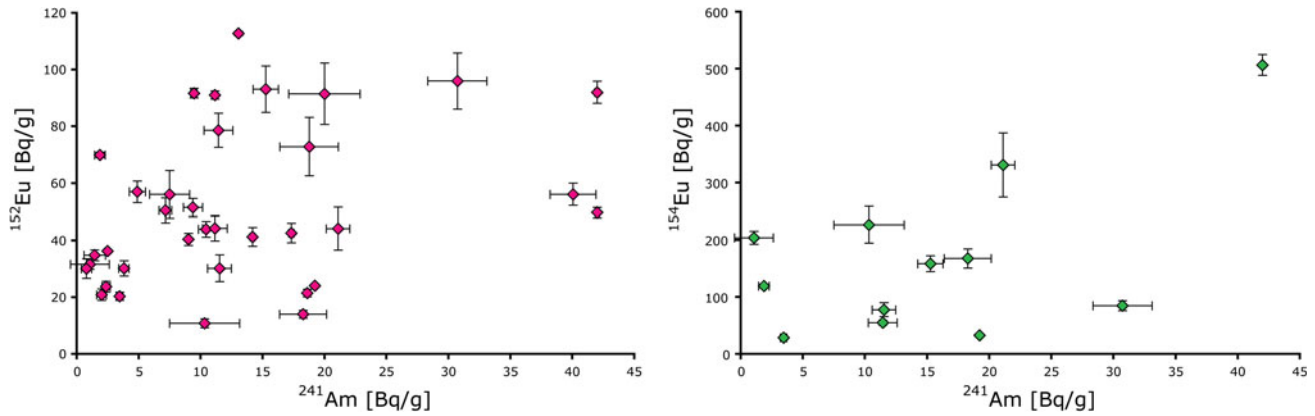

Fig. 3 ^{241}Am versus ^{152}Eu and ^{154}Eu. *Error bars* are 1σ. Units are Bq/g normalized to the time of detonation

therefore, can be approximated with the cadmium ratio for a nuclear reactor [2, 14]. The slow neutron flux is then compared to the measured curve of the slow neutron flux measured by Klema [15] and reported by Bainbridge [9], which yields the absolute distance from the neutron source. The measured slow neutron flux curve of Klema [15] was for a distance over 300 m, and the distances used in this study are an extrapolation from that curve below 300 m, similar to the studies of Belloni et al. [10] and Parekh et al. [2]. The device was located on top of a 30.5 m high tower, and therefore, the absolute distance (from the device) is converted into distance away from ground zero (base of the tower) using the Pythagorean Theorem.

Results

The activities of each isotope, decay-corrected to the time of detonation, and the statistics on the sample population for each isotope are listed in Tables 2 and 3, respectively. The three dominant radioisotopes are ^{137}Cs, ^{152}Eu, and ^{241}Am for the trinitite samples investigated here. ^{154}Eu was observed in 14 of the samples and ^{133}Ba, ^{155}Eu, and ^{239}Pu were detected in either three or four of the samples (Table 4). Additionally, activities for several natural radioisotopes (e.g., ^{40}K, ^{212}Pb, ^{238}U) were recorded but are not reported because they are outside the scope of this study. In contrast to previous studies (i.e., [2, 16]), ^{60}Co, an activation product, was not detected in any of the samples. The range in activities for each of the isotopes investigated here is large (Table 3), but the average activities measured here are comparable to those reported in the literature [2, 10, 16].

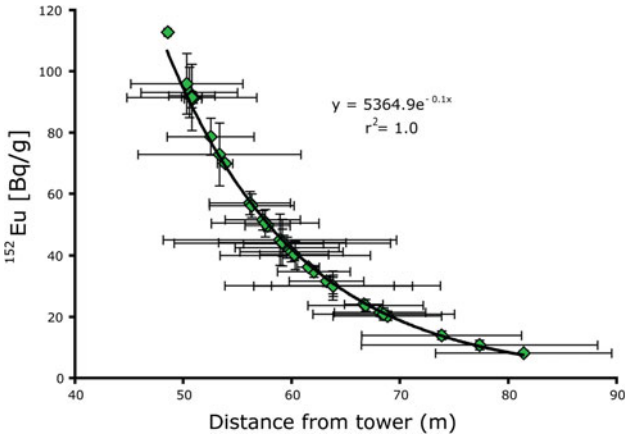

Fig. 4 Activity of ^{152}Eu versus distance away from the base of the tower. *Error bars* are 1σ. Units are Bq/g normalized to the time of detonation

Discussion

Behavior of radioisotopes

The data shown in Fig. 2 yield positive correlations/trends between the activities for several of the isotopes derived from the Gadget. In general, activities for ^{241}Am and ^{137}Cs are correlated (Fig. 2A); however, several of the plots shown in Fig. 2 are based on a small sample set (n = 3 or 4; Fig. 2B, C, D), and therefore, the degree of significance of the correlations is difficult to assess. Moreover, there are essentially no correlations between the activities for ^{241}Am versus ^{133}Ba (Fig. 2D) and the activation products derived from the surrounding sand (^{152}Eu and ^{154}Eu; Fig. 3). The lack of correlation between the activities of the device-derived ^{241}Am and ^{133}Ba renders the origin of the latter ambiguous, and could be the result of multiple source activation of ^{132}Ba (Fig. 2D).

Employing a spatial model

When plotted against calculated distances (Table 4; Figs. 4 and 5), activities for all isotopes define a random scatter, which implies a homogeneous distribution of the nuclides

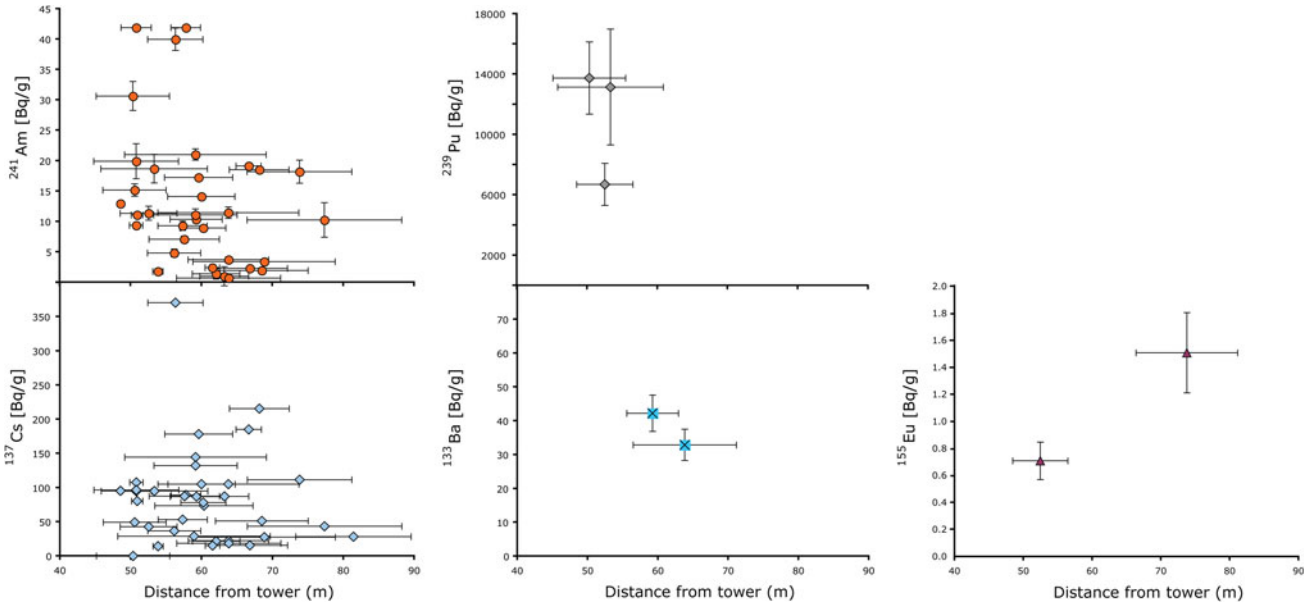

Fig. 5 All isotopes plotted against distance away from the base of the tower. Units are Bq/g normalized to the time of detonation. *Error bars* are 1σ

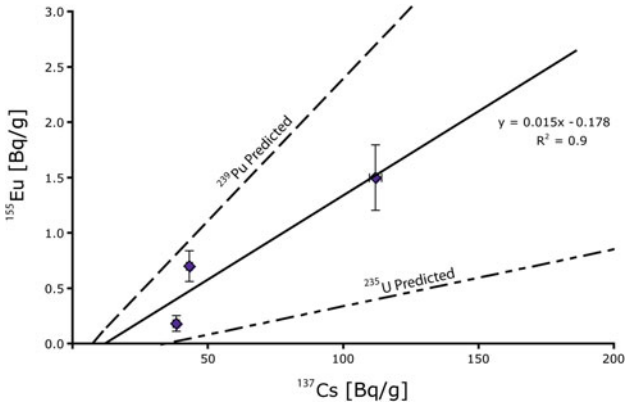

Fig. 6 ^{137}Cs versus ^{155}Eu and predicted ratios of fission products from both the neutron induced fission of ^{239}Pu and ^{235}U from Wahl, [7]. *Error bars* are 1σ. Units are Bq/g normalized to the time of detonation

subsequent detonation. Importantly, ^{241}Am, a daughter product of ^{241}Pu, which has a boiling temperature of 3,232 °C [17] and ^{137}Cs, which is a daughter product of ^{138}Xe ($t_{1/2}$ = 3.8 m), has a boiling temperature of 671 °C [17] do not indicate trends. If temperature-controlled fractionations prevailed, then these would correlate with calculated distances away from the point with the highest temperature, presumably ground zero. However, there is no trend and therefore, it is unlikely that temperature had an effect on the distribution of these isotopes. This result is in contrast with previous studies, which observed depletions in the volatile isotope, ^{137}Cs, in the samples closer to ground zero [2, 10]. Belloni et al. [10] and Parekh et al. [2] focused on a small number of trinitite samples (n = 3), and the fractionations observed in their studies may be the result of sampling bias. Additionally, the samples that lack ^{152}Eu and hence originating even further away from ground zero, display the same range in activity for each isotope as samples located closer to ground zero. This observation corroborates a homogenous distribution for the radioisotopes measured here.

Predicted fission products

Wahl [7] predicted a fission yield for both ^{137}Cs and ^{155}Eu at 6.762 and 0.173 %, respectively, corresponding to an expected ^{155}Eu/^{137}Cs ratio of ~0.03. The calculated ratio of ^{155}Eu/^{137}Cs based on the samples investigated here is 0.012 ± 0.006 (1σ, n = 3). Figure 6 is a plot of the calculated ratios for the fission of ^{239}Pu, ^{235}U, and the activities measured for three samples of trinitite. Fission products for the thermal neutron induced fission of ^{238}U are not available in the literature, but the A number of fission products are determined by the A number of the parent [7]. Therefore, the yields of fission products of ^{238}U should be close to those from the fission of ^{239}Pu. Additionally, fast neutrons (>1 MeV) are needed to induce fission in ^{238}U [18] and these were limited in the Trinity event [2]. Hence, abundant fission of ^{238}U atoms is unlikely. Temperature probably did not play a role in decreasing ^{155}Eu/^{137}Cs, as the boiling point of Eu (1,527 °C, [17]) is significantly higher than that of Cs; therefore, the lack of temperature-controlled fractionations for ^{137}Cs also implies analogously for ^{155}Eu. The observed data do not plot on the line predicted by the fission of ^{239}Pu (~^{238}U), and the decrease in the ^{155}Eu/^{137}Cs ratio is likely the result of the thermal neutron-induced fission products of ^{235}U mixing with those of ^{239}Pu. Semkow et al. [8] modeled that the Trinity test could have up to 30 % fission of U from the natural U tamper. Therefore, these results are consistent with Semkow et al. [8] and indicate mixing between the modeled fission products of both ^{239}Pu and ^{235}U from Wahl [7].

Conclusions

The activities of ^{133}Ba, ^{137}Cs, ^{152}Eu, ^{154}Eu, ^{155}Eu, ^{239}Pu, and ^{241}Am in the largest sample set, to date, of bulk trinitite have been determined using gamma spectroscopy. Based on the relative activities of ^{137}Cs, ^{155}Eu, ^{239}Pu, and ^{241}Am, a similar behavior of these isotopes during the Trinity test is observed. The behavior of ^{133}Ba does not correlate with any of the bomb-derived isotopes, and therefore, its exact origin remains ambiguous.

Based on the activity of ^{152}Eu, a spatial model calculation for the radioisotopes indicates their homogeneous distribution. Lastly, the ratios of fission products ^{155}Eu and ^{137}Cs differ greatly than what is predicted, and these are not related to temperature-controlled fractionations. Therefore, it is possible that the fission components have a ^{235}U signature and, the energy produced in the Trinity test was derived from the fission of both ^{239}Pu and ^{235}U.

Acknowledgments The authors thank the separations and radiochemistry research team at Pacific Northwest National Laboratory and Dr. Ed Stech in the Department of Physics at the University of Notre Dame for thoughtful discussions. This research work was funded by DOE/NNSA grant PDP11-40/DE-NA0001112.

References

1. Fahey AJ, Zeissler CJ, Newbury DE, Davis J, Lindstrom RM (2010) Postdetonation nuclear debris for attribution. Proc Nat Acad Sci 107(47):20207–20212
2. Parekh PP, Semkow TM, Torres MA, Haines DK, Cooper JM, Rosenburg PM, Kitto ME (2006) Radioactivity in trinitite six decades later. J Environ Radioact 85:103–120
3. Eby N, Hermes R, Charnley N, Smoliga JA (2010) Trinitite-the atomic rock. Geol Today 26(5):180–185

4. Staritzky E (1950) Thermal effects of atomic bomb explosions on soils at Trinity and Eniwetok. Los Alamos Scientific Laboratory, LA-1126, p 21
5. Storms B (1965) Trinity. The Atom 2(8):1–34
6. Rhodes R (1986) The making of the atomic bomb, 1st edn. Simon and Schuster, New York, pp 575–577, 657
7. Wahl AC (1988) Nuclear-charge distribution and delayed-neutron yields for thermal-neutron-induced fission of ^{235}U, ^{233}U, and ^{239}Pu and for spontaneous fission of ^{252}Cf. At Data Nucl Data Tables 39:1–156
8. Semkow TM, Parekh PP, Haines DK (2006) Modeling the effects of the trinity test. Appl Model Comput Nucl Sci 945:142–159
9. Bainbridge KT (1976) Trinity Report LA-6300-H. Los Alamos Scientific Laboratory, Los Alamos
10. Belloni F, Himbert J, Marzocchi O, Romanello V (2011) Investigating incorporation and distribution of radionuclides in trinitite. J Environ Radioact 102:852–862
11. Love DW, Allen BD, Myers RG (2008) Gypsum crystal morphologies and diverse accumulations of gypsum and other evaporites in the Tularosa basin. New Mexico Geol 30:120–121
12. Bellucci JJ, Simonetti A (2012) Nuclear forensics: searching for nuclear device debris in trinitite-hosted inclusions. J Radioanal Nucl Chem 293:313–319
13. US GPO (2000) Trinity site July 16, 1945. US Government Printing Office: 2000–844-916, Washington DC
14. Brunfelt AO, Roelandts I, Steinnes E (1977) Some new methods for the determination of rare-earth elements in geological materials using thermal and epithermal neutron activation. J Radioanal Chem 38:451–459
15. Klema ED (1945) July 16th nuclear explosion: neutron measurements with gold-foil detectors. Los Alamos Scientific Laboratory report, LA-362
16. Schlauf D, Siemon K, Weber R, Esterlund RA, Molzahn D, Parzelt P (1997) Trinitite redux: comment of "Determining the yield of the Trinity nuclear device via gamma-ray spectroscopy" by David Arkatz and Christopher Bragg. American Journal of Physics. 65(11), 1110–112. Am J Phys 63:411–413
17. Liede DR (ed) (2003) CRC handbook of chemistry and physics, 84th edn. CRC Press, Boca Raton
18. Shoupp WE, Hill JE (1949) Thresholds for fast neutron fission in thorium and uranium. Phys Rev 75(5):785–789